Published in final edited form as:
Nat Cell Biol. 2013 November ; 15(11): 1370–1377. doi:10.1038/ncb2842.

Kinetic framework of spindle assembly checkpoint signaling

Amalie E. Dick[1,2,3] and **Daniel W. Gerlich**[1,2,3,*]

[1]Institute of Molecular Biotechnology of the Austrian Academy of Sciences (IMBA), 1030 Vienna, Austria [2]Institute of Biochemistry, ETH Zurich, 8093 Zurich, Switzerland [3]Marine Biological Laboratory, Woods Hole, MA 02543, USA

Abstract

The mitotic spindle assembly checkpoint (SAC) delays anaphase onset until all chromosomes have attached to both spindle poles[1,2]. Here, we investigated SAC signaling kinetics in response to acute detachment of individual chromosomes using laser microsurgery. Most detached chromosomes delayed anaphase until they had realigned to the metaphase plate. A substantial fraction of cells, however, entered anaphase in the presence of unaligned chromosomes. We identify two mechanisms by which cells can bypass the SAC: First, single unattached chromosomes inhibit the anaphase promoting complex/cyclosome (APC/C) less efficiently than a full complement of unattached chromosomes. Second, because of the relatively slow kinetics of reimposing APC/C inhibition during metaphase, cells were unresponsive to chromosome detachment up to several minutes before anaphase onset. Our study defines when cells irreversibly commit to enter anaphase and shows that the SAC signal strength correlates with the number of unattached chromosomes. Detailed knowledge about SAC signaling kinetics is important for understanding the emergence of aneuploidy and the response of cancer cells to chemotherapeutics targeting the mitotic spindle.

Spindle assembly is an error prone process, which can involve multiple rounds of microtubule attachment and detachment on individual kinetochores[3, 4]. Incorrectly attached chromosomes, for example when both sister kinetochores bind to the same spindle pole, are detected by an error correction machinery, which depolymerizes microtubules on kinetochores if they are under low mechanical tension (reviewed in [5]). This enables chromosomes to eventually attach their sister kinetochores to microtubules originating from opposing spindle poles.

Due to the stochastic nature of spindle assembly, anaphase must be robustly delayed when individual chromosomes fail to attach properly. Indeed, a single unattached kinetochore can delay anaphase onset for up to several hours in PtK_1 cells[6]. Yet, even when all kinetochores are unattached by drug-induced depolymerization of microtubules, cyclin B continues to be degraded by low residual APC/C activity, which leads to mitotic exit in presence of an

*Address correspondence to DWG. daniel.gerlich@imba.oeaw.ac.at.
Author contributions: A.E.D. designed and conducted experiments and analyzed data. D.W.G. conceived the project, analyzed data, and wrote the manuscript with help by A.E.D.

Competing financial interests: The authors declare no competing financial interests.

Europe PMC Funders Author Manuscripts

active SAC (mitotic slippage)[7-9]. Mitotic slippage occurs at different rates in a variety of cancer and non-cancer cells and it has been proposed as a mechanism by which cancer cells may develop resistance against therapeutics that target the mitotic spindle[8-12]. Hence, it is important to better understand the signaling kinetics underlying SAC-mediated APC/C inhibition.

Unattached kinetochores recruit the SAC protein Mad2 to promote assembly of cytoplasmic mitotic checkpoint complex, composed of Mad2, Bub3, BubR1, and Cdc20 (reviewed in [1, 2]). The mitotic checkpoint complex suppresses anaphase entry by inhibiting APC/C binding to metaphase substrates like cyclin B and securin. Current models posit that continuous turnover of mitotic checkpoint complex on APC/C by Cdc20 autoubiquitylation enables rapid response of the SAC to the chromosome attachment status, as it liberates APC/C to bind free Cdc20 once the SAC has been satisfied[13-18].

Little is known about the kinetics and efficiency by which the SAC and the APC/C respond to individual chromosome attachment or detachment events. We therefore set out to measure SAC signaling in live cells, using quantitative microscopy and biophysical spindle perturbations.

To study the kinetics by which cells mount a SAC signal, we developed a laser microsurgery procedure for acute detachment of kinetochore fibers from individual chromosomes. HeLa cells stably expressing the chromatin marker histone 2B (H2B) tagged with mCherry, and the spindle marker mEGFP-α-tubulin were cut by a high-energy pulsed laser on microtubules at the edge of the mitotic spindle (Fig. 1a). This released one (n = 20 cells) or few (n = 15 cells) chromosomes from the metaphase plate. The displaced chromosomes always moved towards the spindle pole opposing the site of the cut, presumably driven by pulling forces generated at the sister kinetochore that remained connected to the spindle.

We next investigated how laser microsurgery affected the kinetochore-microtubule interface. To determine the SAC signaling state on laser-detached chromosomes we used HeLa cells stably expressing mouse Mad2-EGFP from its endogenous promoter and H2B-mCherry. Mouse Mad2-EGFP is functional in HeLa cells, as it effectively restored a nocodazole-induced arrest after RNAi-mediated depletion of the endogenous human Mad2 (Supplementary Fig. S1a-c). Following laser microsurgery and live-cell imaging (Fig. 1b, Supplementary Fig. S1d), we fixed cells for correlative microtubule immunofluorescence staining (Fig. 1c, Supplementary Fig. S1e). 27 chromosomes were displaced from metaphase spindles in 18 cells, and all displaced chromosomes had accumulated Mad2-EGFP at the time of fixation (2:20 to 6:00 min:s after laser microsurgery), either on a pair of dots (18 chromosomes; Fig. 1c, d) or on a single dot (9 chromosomes; Fig. 1e, Supplementary Fig. S1d, e). This indicates that laser microsurgery efficiently induces SAC signaling on displaced chromosomes.

Previous work indicates that monotelically attached kinetochores can accumulate low levels of Mad2[19]. Most laser-displaced chromosomes accumulated Mad2-EGFP to similarly high levels on both sister kinetochores (Supplementary Fig. S1f), suggesting that laser microsurgery had completely detached the respective chromosomes. This is unlikely to be

caused by kinetochore damage given the proficiency in Mad2-EGFP accumulation. Rather, we suspect that a drop in mechanical tension between sister kinetochores may have stimulated microtubule disassembly on both sister kinetochores by the error correction machinery[5]. Monotelic chromosomes induced by laser microsurgery thus appear to be less stably attached to microtubules compared to previously observed spontaneously occurring monotelic chromosome attachments[6]. A possible explanation for this may be the dissociation of Polo like kinase 1 (Plk1) from kinetochores when chromosomes have aligned on the metaphase plate[20, 21]. This changes the microtubule-kinetochore interface from a state that favors initial stable interactions to a more dynamic attachment state that enables efficient attachment error correction during metaphase[21].

Following laser microsurgery, most chromosomes moved along the edge of the spindle. The high microtubule density at these regions precluded a comprehensive analysis of chromosome interactions with microtubules by immunofluorescence microscopy and we therefore focused our analysis on Mad2-positive kinetochores. 31 out of 45 Mad-EGFP dots on laser-displaced chromosomes localized just at the edge of the spindle (Fig. 1c, d), consistent with previously observed abundant lateral microtubule interactions of unattached kinetochores in unperturbed mitosis[4, 22]. 14 Mad2-EGFP dots on unaligned chromosomes localized away from high microtubule density regions, of which 3 Mad2-EGFP dots appeared unattached, whereas 11 Mad2-EGFP dots appeared to interact laterally with faintly stained astral microtubules (Fig. 1d, e). End-on attachments of microtubules to laser-displaced chromosomes, in contrast, were never observed at Mad2-EGFP dots, yet we did detect end-on attachments at chromosome regions opposing single Mad2-EGFP dots (Fig. 1e). Taking the Mad2-EGFP and microtubule localization data together, we conclude that laser microsurgery destabilizes end-on microtubule attachments on displaced chromosomes to induce SAC signaling on one or two sister kinetochores (Fig. 1f).

We next investigated how laser microsurgery affected mitotic progression in HeLa cells (Fig. 2). In the majority of cells (23 of 35), laser-displaced chromosomes were recaptured by the spindle and recongressed to the metaphase plate during the imaging period of 40 min after cutting. 16 out of 23 cells that had recongressed laser-displaced chromosomes entered anaphase within 40 min after laser microsurgery, yet with significant delay compared to control cells, in which laser microsurgery was performed in regions adjacent to the metaphase spindle (n = 21 cells; Fig. 2a, d; Supplementary Video 1; control cells: 8:59 min:s (median); Fig. 2b, d; Supplementary Video 2; anaphase entry after chromosome displacement and recongression: 30:22 min:s (median); $p = 8.8 * 10^{-6}$ by Mann-Whitney U-test). Thus, SAC-mediated anaphase delay and recapture by the spindle corrected acute laser-detachment of chromosomes in the majority of cells.

Surprisingly, 11 out of 35 cells entered anaphase in the presence of unaligned chromosomes (Fig. 2c, d; Supplementary Video 3). This is a much higher mitotic slippage rate compared to cells treated with microtubule-depolymerizing drugs: in presence of 100 ng/ml nocodazole, mitotic slippage was never observed within 10 h and it occurred only after 19:09 h:min (median; n = 50 cells). Anaphase entry in presence of unaligned chromosomes occurred with comparable incidence in laser-microsurgery experiments using non-transformed retinal pigmental epithelial cells that have been immortalized by stable

overexpression of human telomerase reverse transcriptase (hTERT-RPE1 cells; Supplementary Fig. S2). Thus, a substantial fraction of laser-detached chromosomes bypasses SAC surveillance in cancerous and non-cancerous cells.

What causes the high incidence of mitotic slippage in presence of single unattached chromosomes? One possibility is that the SAC may not re-impose APC/C inhibition fast enough to halt cells once they have progressed to late metaphase stages. Alternatively, single unattached chromosomes may inhibit the APC/C less efficiently than a full complement of unattached chromosomes. This may lead to accelerated mitotic slippage, although it seems unlikely that mitotic slippage can occur within an observation time of less than an hour, given that HeLa cells can arrest for several hours in response to small numbers of unaligned chromosomes[23]. To test these hypotheses, we developed assays to measure the response time and inhibitory strength of the SAC.

To determine how fast a SAC signal is mounted, we measured Mad2 accumulation kinetics in cells stably expressing Mad2-EGFP and H2B-mCherry (Fig. 3a, b; Supplementary Video 4). Mad2-EGFP was first detected on displaced chromosomes 88 ± 39 s (mean ± s.d.; n = 16 cells) after laser microsurgery and reached plateau levels at ~3-4 min (Fig. 3b). Peak levels of Mad2-EGFP on laser-detached chromosomes were similar to those on chromosomes of cells treated with 100 or 500 ng/ml nocodazole (Fig. 3c). Thus, laser-microsurgery leads to fast and efficient recruitment of Mad2 on displaced chromosomes. The relatively high variability observed for Mad2-EGFP recruitment onset could reflect measurement noise owing to the low signal intensities of Mad2-EGFP. It is also possible that mounting a SAC signal on individual kinetochores involves a stochastic process or that Mad2-EGFP accumulation becomes less efficient when cells progress to late stages of metaphase.

We next investigated how fast the APC/C responds to laser microsurgery, by measuring degradation of its fluorescent substrate securin-mEGFP[24, 25], stably expressed in HeLa cells together with H2B-mCherry[25]. Degradation of EGFP-tagged securin correlates well with that of endogenous securin[24] and stable expression of securin-mEGFP does not perturb mitotic progression[25]. Laser displacement of chromosomes in metaphase cells, which had already started to degrade securin-mEGFP, strongly reduced APC/C activity in 9 out of 11 cells (Fig. 4a, c; Supplementary Fig. S3 and S4; Supplementary Video 5). Significant APC/C inhibition in these cells, however, occurred only after a lag-phase of >5 min (Fig. 4c, e; $p = 1.1 * 10^{-3}$ by t-test with Welch's correction). Two cells entered anaphase shortly after laser microsurgery in presence of unaligned chromosomes and without detectable reduction of securin-mEGFP degradation (Fig. 4b, d; Supplementary Fig. S4; Supplementary Video 6), possibly because they lacked sufficient time to re-impose APC/C inhibition. Previous studies showed that the SAC is inactive during anaphase, when tension is low on kinetochores due to loss of cohesion[26, 27]. Our data indicate that the APC/C becomes unresponsive to chromosome detachment already ~5 min prior to anaphase onset. This marks an irreversible point-of-no-return to exit mitosis and it reveals that SAC inactivation is scheduled before cohesin cleavage, which initiates about 2-3 min prior to anaphase onset[28, 29].

Next, we investigated the extent by which laser-detached chromosomes inhibited the APC/C. At 5-10 min after laser-mediated chromosome displacement, securin-mEGFP was degraded at a rate of 0.60 ± 0.10 %/min (mean ± s.e.m.; n = 9 cells; Fig. 4e). For comparison, we measured the full dynamic range of APC/C activity. Peak activity of APC/C was determined in untreated control cells and in cells depleted of Mad2 by RNAi briefly before the metaphase-anaphase transition (Fig. 5a, c). Securin-mEGFP degraded at a rate of 4.8 ± 0.24 %/min (mean ± s.e.m.) in control cells (n = 10 cells), which was similar to Mad2 RNAi cells (4.8 ± 0.22 %/min; n = 10 cells). Spindle disruption by 100 ng/ml nocodazole strongly inhibited the APC/C to a residual securin-mEGFP degradation rate of 0.085 ± 0.007 %/min (mean ± s.e.m.; n = 10 cells; Fig. 5b, c). Hence, in HeLa cells the SAC has the capacity to impose a ~60-fold inhibition on the APC/C and individual chromosomes inhibited the APC/C significantly less efficiently than complete spindle disruption ($p = 8.3 * 10^{-4}$ by t-test with Welch's correction).

Because APC/C inhibition may not have reached its full extent 5-10 min after chromosome detachment, we aimed to measure APC/C activity for longer time durations. As most laser-displaced chromosomes realigned to the metaphase plate within short time, we searched for an alternative method to induce persistent Mad2 signaling from a small number of kinetochores. We therefore titrated nocodazole to low concentrations (6 - 25 ng/ml) that allowed metaphase plate alignment but induced small numbers of unaligned chromosomes. To test if unaligned chromosomes mounted a SAC signal, we performed immunofluorescence staining for Mad2 (Fig. 5d, e). In 34 cells with metaphase plates we detected 65 unaligned chromosomes, of which 64 contained bright Mad2 dots, either on one sister kinetochore (Fig. 5d; 27 unaligned chromosomes) or on both sister kinetochores (Fig. 5e; 37 unaligned chromosomes). In contrast, Mad2 did not accumulate on kinetochores of chromosomes aligned on the metaphase plate in 29 cells (5 cells contained one to three weak Mad2 spots on the metaphase plate). Pearson correlation analysis confirms a high correlation between the number of unaligned chromosomes and the number of Mad2-positive kinetochores (r = 0.81; n = 34 cells).

We next investigated whether APC/C inhibition correlates with the number of unaligned chromosomes (Fig. 5f-h; Supplementary Fig. S5). In presence of a single unaligned chromosome, securin-mEGFP was degraded at 0.32 ± 0.03 %/min (mean ± s.e.m; n = 15 cells), which is significantly faster than in cells treated with 100 ng/ml nocodazole (Fig. 5h; $p = 5.6 * 10^{-7}$ by t-test with Welch's correction). In presence of 2-5 unaligned chromosomes, securin-mEGFP was degraded at intermediate rates, whereas in presence of more than 5 unaligned chromosomes degradation rates were similar to those observed in cells treated with 100 ng/ml nocodazole (Fig. 5g, h). These data confirm that a single unattached chromosome can delay anaphase for several hours as previously observed in PtK_1 cells[6]. However, single unaligned chromosomes do not mount a SAC with full inhibitory strength even though they efficiently accumulate Mad2. This results in substantially faster mitotic slippage compared to conditions where all chromosomes are detached from the spindle. Thus, we conclude that the SAC signal is graded and that its inhibitory strength correlates with the number of Mad2-positive kinetochores. This is counter the prevailing view that the SAC functions as a digital switch that is either in an "on" or "off" state.

Aneuploidy and genomic instability are hallmarks of human cancer[30,31]. Previous studies proposed that merotelic chromosomes, which satisfy the SAC even though they cannot segregate properly, provide a main source of single chromosome aneuploidy[30, 32, 33]. We show that individual unattached or monotelically misattached chromosomes are also prone for missegregation - if they persist for more than 2-3 hours or if they emerge during late metaphase.

The graded response in SAC signaling raises the possibility that an increase in cytoplasmic volume could impair the efficiency of APC/C inhibition per unattached kinetochore. This may be relevant for early divisions of large embryonic cells with weak SAC response[34, 35]. The experimental framework established by our study provides an opportunity to test in future studies whether an increase in cell size can exhaust the SAC signal.

Supplementary Material

Refer to Web version on PubMed Central for supplementary material.

Acknowledgments

The authors thank M. Petronczki and L. Vazquez-Novelle for critical comments on the manuscript, A. Hyman and I. Poser for providing cells expressing Mad2-EGFP, the IMBA-IMP BioOptics core facility and the MBL central microscopy facility for excellent technical support, M. Terasaki, J.M. Peters, P. Meraldi for helpful discussions, and C. Sommer for statistical consultation. Research in the Gerlich laboratory has received funding from the European Community's Seventh Framework Programme FP7/2007-2013 under grant agreements no 241548 (MitoSys) and no 258068 (Systems Microscopy), from an ERC Starting Grant (agreement no 281198), from the EMBO Young Investigator Programme, from the Swiss National Science Foundation, from the Austrian Science Fund (FWF)-funded project "SFB Chromosome Dynamics", and from a Summer Research Award of the Marine Biology Laboratory Woods Hole (Laura and Arthur Colwin Endowed Summer Research Fellowship Fund). A.E.D. is a fellow of the Zurich Ph.D. Program in Molecular Life Sciences and has received funding from a PhD fellowship by the Boehringer Ingelheim Fonds and from a Peter Müller fellowship.

References

1. Musacchio A, Salmon ED. The spindle-assembly checkpoint in space and time. Nat Rev Mol Cell Biol. 2007; 8:379–393. [PubMed: 17426725]
2. Lara-Gonzalez P, Westhorpe FG, Taylor SS. The spindle assembly checkpoint. Curr Biol. 2012; 22:R966–980. [PubMed: 23174302]
3. Kitajima TS, Ohsugi M, Ellenberg J. Complete kinetochore tracking reveals error-prone homologous chromosome biorientation in mammalian oocytes. Cell. 2011; 146:568–581. [PubMed: 21854982]
4. Magidson V, et al. The spatial arrangement of chromosomes during prometaphase facilitates spindle assembly. Cell. 2011; 146:555–567. [PubMed: 21854981]
5. Lampson MA, Cheeseman IM. Sensing centromere tension: Aurora B and the regulation of kinetochore function. Trends Cell Biol. 2011; 21:133–140. [PubMed: 21106376]
6. Rieder CL, Cole RW, Khodjakov A, Sluder G. The checkpoint delaying anaphase in response to chromosome monoorientation is mediated by an inhibitory signal produced by unattached kinetochores. J Cell Biol. 1995; 130:941–948. [PubMed: 7642709]
7. Brito DA, Rieder CL. Mitotic checkpoint slippage in humans occurs via cyclin B destruction in the presence of an active checkpoint. Curr Biol. 2006; 16:1194–1200. [PubMed: 16782009]
8. Rieder CL, Maiato H. Stuck in Division or Passing through; What Happens When Cells Cannot Satisfy the Spindle Assembly Checkpoint. Dev Cell. 2004; 7:637–651. [PubMed: 15525526]

9. Manchado E, et al. Targeting mitotic exit leads to tumor regression in vivo: Modulation by Cdk1, Mastl, and the PP2A/B55alpha,delta phosphatase. Cancer Cell. 2010; 18:641–654. [PubMed: 21156286]
10. Gascoigne KE, Taylor SS. How do anti-mitotic drugs kill cancer cells? J Cell Sci. 2009; 122:2579–2585. [PubMed: 19625502]
11. Huang HC, Shi J, Orth JD, Mitchison TJ. Evidence that mitotic exit is a better cancer therapeutic target than spindle assembly. Cancer Cell. 2009; 16:347–358. [PubMed: 19800579]
12. Yang Z, Kenny AE, Brito DA, Rieder CL. Cells satisfy the mitotic checkpoint in Taxol, and do so faster in concentrations that stabilize syntelic attachments. J Cell Biol. 2009; 186:675–684. [PubMed: 19720871]
13. Reddy SK, Rape M, Margansky WA, Kirschner MW. Ubiquitination by the anaphase-promoting complex drives spindle checkpoint inactivation. Nature. 2007; 446:921–925. [PubMed: 17443186]
14. Nilsson J, Yekezare M, Minshull J, Pines J. The APC/C maintains the spindle assembly checkpoint by targeting Cdc20 for destruction. Nat Cell Biol. 2008; 10:1411–1420. [PubMed: 18997788]
15. Uzunova K, et al. APC15 mediates CDC20 autoubiquitylation by APC/C(MCC) and disassembly of the mitotic checkpoint complex. Nat Struct Mol Biol. 2012; 19:1116–1123. [PubMed: 23007861]
16. Mansfeld J, Collin P, Collins MO, Choudhary JS, Pines J. APC15 drives the turnover of MCC-CDC20 to make the spindle assembly checkpoint responsive to kinetochore attachment. Nat Cell Biol. 2011; 13:1234–1243. [PubMed: 21926987]
17. Foster SA, Morgan DO. The APC/C subunit Mnd2/Apc15 promotes Cdc20 autoubiquitination and spindle assembly checkpoint inactivation. Mol Cell. 2012; 47:921–932. [PubMed: 22940250]
18. Varetti G, Guida C, Santaguida S, Chiroli E, Musacchio A. Homeostatic control of mitotic arrest. Mol Cell. 2011; 44:710–720. [PubMed: 22152475]
19. Waters JC, Chen RH, Murray AW, Salmon ED. Localization of Mad2 to kinetochores depends on microtubule attachment, not tension. J Cell Biol. 1998; 141:1181–1191. [PubMed: 9606210]
20. Lenart P, et al. The small-molecule inhibitor BI 2536 reveals novel insights into mitotic roles of polo-like kinase 1. Curr Biol. 2007; 17:304–315. [PubMed: 17291761]
21. Liu D, Davydenko O, Lampson MA. Polo-like kinase-1 regulates kinetochore-microtubule dynamics and spindle checkpoint silencing. J Cell Biol. 2012; 198:491–499. [PubMed: 22908307]
22. Kapoor TM, et al. Chromosomes can congress to the metaphase plate before biorientation. Science. 2006; 311:388–391. [PubMed: 16424343]
23. Stevens D, Gassmann R, Oegema K, Desai A. Uncoordinated loss of chromatid cohesion is a common outcome of extended metaphase arrest. PLoS One. 2011; 6:e22969. [PubMed: 21829677]
24. Hagting A, et al. Human securin proteolysis is controlled by the spindle checkpoint and reveals when the APC/C switches from activation by Cdc20 to Cdh1. J Cell Biol. 2002; 157:1125–1137. [PubMed: 12070128]
25. Held M, et al. CellCognition: time-resolved phenotype annotation in high-throughput live cell imaging. Nat Methods. 2010; 7:747–754. [PubMed: 20693996]
26. Vazquez-Novelle MD, Petronczki M. Relocation of the chromosomal passenger complex prevents mitotic checkpoint engagement at anaphase. Curr Biol. 2010; 20:1402–1407. [PubMed: 20619651]
27. Mirchenko L, Uhlmann F. Sli15(INCENP) dephosphorylation prevents mitotic checkpoint reengagement due to loss of tension at anaphase onset. Curr Biol. 2010; 20:1396–1401. [PubMed: 20619650]
28. Gerlich D, Koch B, Dupeux F, Peters JM, Ellenberg J. Live-cell imaging reveals a stable cohesin-chromatin interaction after but not before DNA replication. Curr Biol. 2006; 16:1571–1578. [PubMed: 16890534]
29. Shindo N, Kumada K, Hirota T. Separase sensor reveals dual roles for separase coordinating cohesin cleavage and cdk1 inhibition. Dev Cell. 2012; 23:112–123. [PubMed: 22814604]
30. Gordon DJ, Resio B, Pellman D. Causes and consequences of aneuploidy in cancer. Nat Rev Genet. 2012; 13:189–203. [PubMed: 22269907]
31. Holland AJ, Cleveland DW. Boveri revisited: chromosomal instability, aneuploidy and tumorigenesis. Nat Rev Mol Cell Biol. 2009; 10:478–487. [PubMed: 19546858]

32. Cimini D, et al. Merotelic kinetochore orientation is a major mechanism of aneuploidy in mitotic mammalian tissue cells. J Cell Biol. 2001; 153:517–527. [PubMed: 11331303]
33. Thompson SL, Compton DA. Examining the link between chromosomal instability and aneuploidy in human cells. J Cell Biol. 2008; 180:665–672. [PubMed: 18283116]
34. Glover DM. Mitosis in the Drosophila embryo--in and out of control. Trends Genet. 1991; 7:125–132. [PubMed: 2068783]
35. Sluder G. Role of spindle microtubules in the control of cell cycle timing. J Cell Biol. 1979; 80:674–691. [PubMed: 572367]

Europe PMC Funders Author Manuscripts

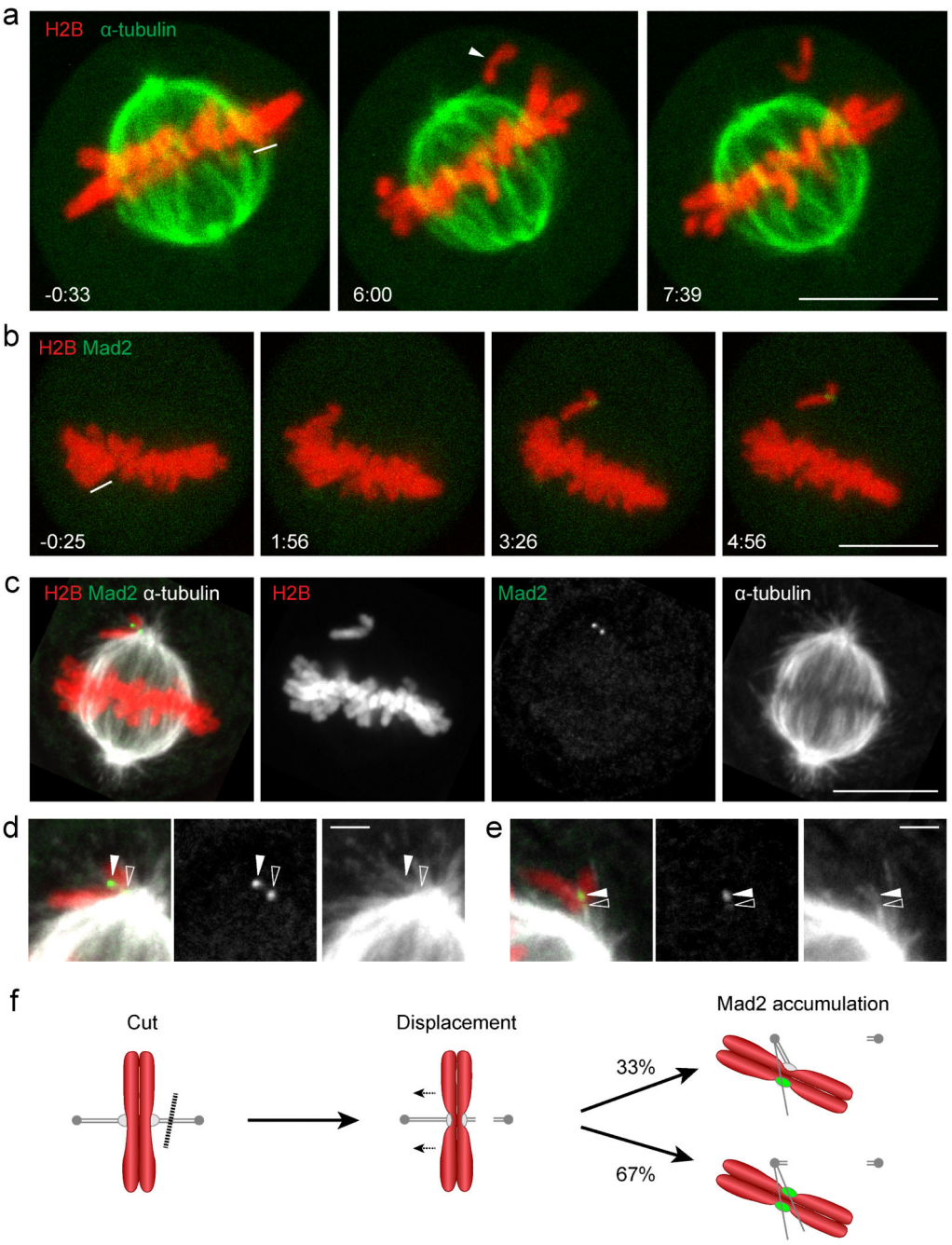

Figure 1. Laser microsurgery of kinetochore fibers induces Mad2 accumulation on individual displaced chromosomes

(**a**) A live metaphase HeLa cell expressing H2B-mCherry and mEGFP-α-tubulin was imaged by 3D-confocal live-cell microscopy. Kinetochore fiber microtubules were cut with a pulsed 915 nm laser at the area indicated by the white line. The arrowhead indicates a single unaligned chromosome. (**b-e**) Correlative laser microsurgery, time-lapse imaging, and immunofluorescence staining of the spindle. (**b**) A live metaphase HeLa cell expressing H2B-mCherry and Mad2-EGFP was cut with a pulsed 915 nm laser at the area indicated by

the white line, and imaged by 3D-confocal live-cell microscopy. (**c**) The cell shown in (b) was fixed 6 min after laser microsurgery and stained for α-tubulin. (**d**) Enlarged region of (c) with linearly increased contrast to enhance visualization of astral microtubules. This reveals lateral microtubule association of a Mad2-positive kinetochore (closed arrowhead), and its sister kinetochore (open arrowhead) localizing to the edge of the spindle. (**e**) Example for unaligned chromosome with single Mad2 accumulation site (solid arrowhead), 2:20 min:s after laser microsurgery (see Supplementary Fig. S1d, e for time-lapse images and overview of cell). The contrast was linearly increased to visualize astral microtubules. Open arrowhead indicates end-on attachment of a microtubule bundle at a chromosome region opposite of the Mad2-positive kinetochore. (**f**) Schematic overview of the laser microsurgery assay. Chromosomes (red), microtubules, kinetochores (gray), and Mad2 (green). Dashed line indicates laser microsurgery. Time = 0:00 min:s at the first image acquired immediately after laser microsurgery. Bars: 10 μm (a-c); 2 μm (d, e).

Europe PMC Funders Author Manuscripts

Europe PMC Funders Author Manuscripts

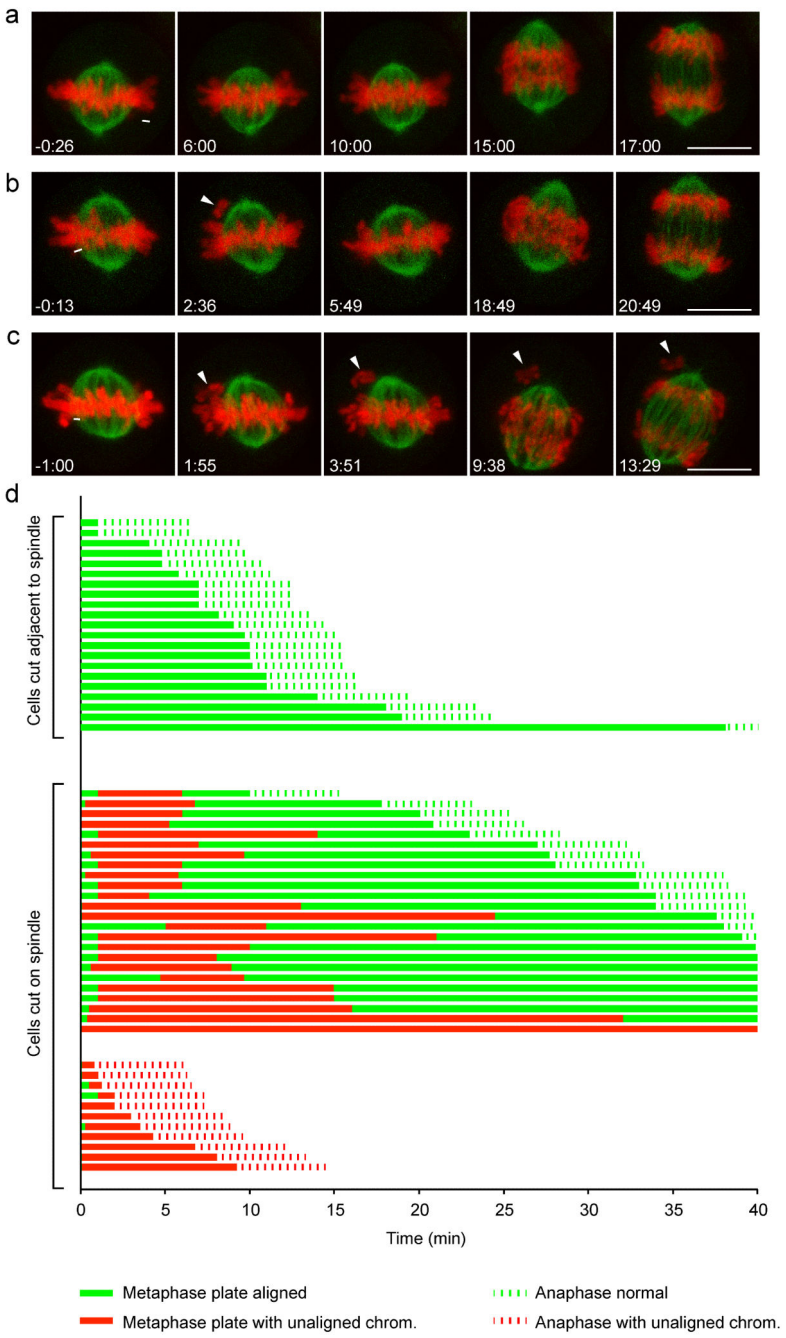

Figure 2. Fate of cells after laser-induced chromosome detachment

HeLa cells expressing H2B-mCherry and mEGFP-α-tubulin were imaged for 40 min by 3D-confocal live-cell microscopy and cut with a pulsed 915 nm laser at the area indicated by the white lines. Time = 0:00 min:s at the first image acquired immediately after laser microsurgery. (**a**) A representative control cell was cut in a region adjacent to the spindle so that no chromosome was detached. (**b**) A representative cell in which a single chromosome was detached from the mitotic spindle by laser microsurgery. The arrowhead indicates the detached chromosome (2:36), which subsequently recongresses to the metaphase plate

(5:49). (**c**) As in (b), but this cell enters anaphase in the presence of an unaligned chromosome (arrowheads). Bars: 10 μm. (**d**) Fate trajectories of 56 cells cut by laser microsurgery. 21 control cells were cut as in (a), and 35 cells were cut as in (b, c).

Europe PMC Funders Author Manuscripts

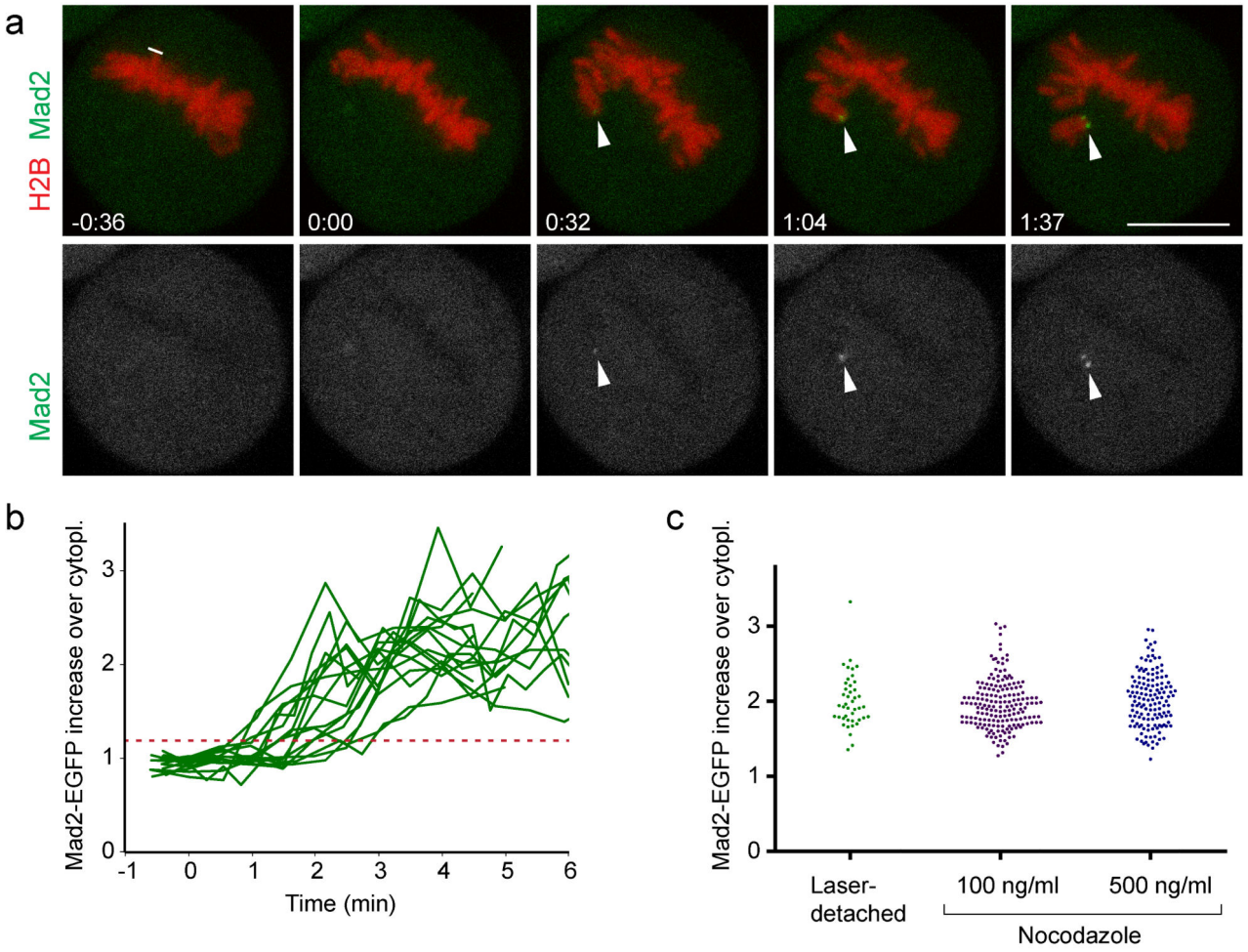

Figure 3. SAC response kinetics after laser microsurgery

(**a**) A live metaphase HeLa cell expressing H2B-mCherry and Mad2-EGFP was imaged by 3D-confocal live-cell microscopy and cut with a pulsed 915 nm laser at the area indicated by the white line. Arrowheads indicate site of Mad2-EGFP accumulations on the displaced chromosome. Time = 0:00 min:s at the first image acquired immediately after laser microsurgery. Bar: 10 μm. (**b**) Kinetics of Mad2-EGFP enrichment on detached chromosomes, measured in a circular region with a diameter of 1.2 μm (n = 16 cells). Each curve represents the sister kinetochore with the first Mad2-EGFP accumulation. Red dashed line indicates 3 s.d. above the mean Mad2-EGFP fluorescence on chromosomes before cutting, which served as threshold to detect the onset of Mad2-EGFP accumulation. (**c**) Peak levels of Mad2-EGFP were measured at 4:30 - 5:00 min:s after laser microsurgery, or after spindle depolymerization by nocodazole. Each dot represents one kinetochore.

Europe PMC Funders Author Manuscripts

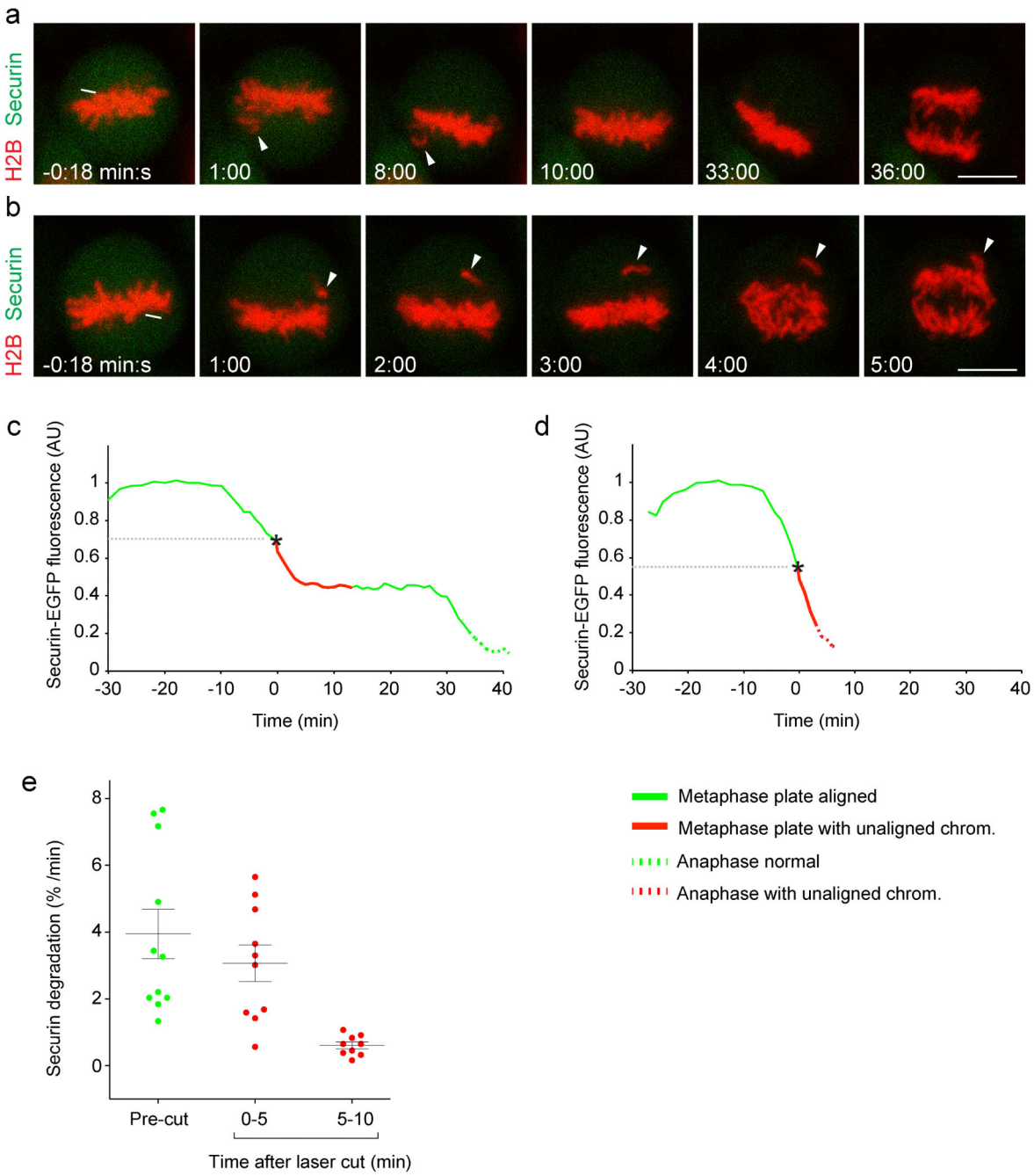

Figure 4. Kinetics of APC/C inhibition after laser microsurgery

HeLa cells expressing H2B-mCherry and securin-mEGFP were imaged by 3D-confocal microscopy from prophase until metaphase. At different time points during metaphase, the spindle was cut by a pulsed 915 nm laser as indicated by the white line. Time = 0:00 min:s at the first image acquired immediately after laser microsurgery. (**a**) A representative cell in which a detached chromosome (arrowheads) recongressed to the metaphase plate before anaphase entry. (**b**) A cell that enters anaphase in presence of an unaligned chromosome (arrowheads). Bars: 10 μm. (**c, d**) Securin-mEGFP degradation kinetics, normalized to

metaphase onset, for the cells shown in (a) or (b), respectively. (**e**) Securin degradation rate was determined by linear interpolation in 11 cells, either before or at different time intervals after laser microsurgery. Error bars indicate mean ± s.e.m.

Europe PMC Funders Author Manuscripts

Europe PMC Funders Author Manuscripts

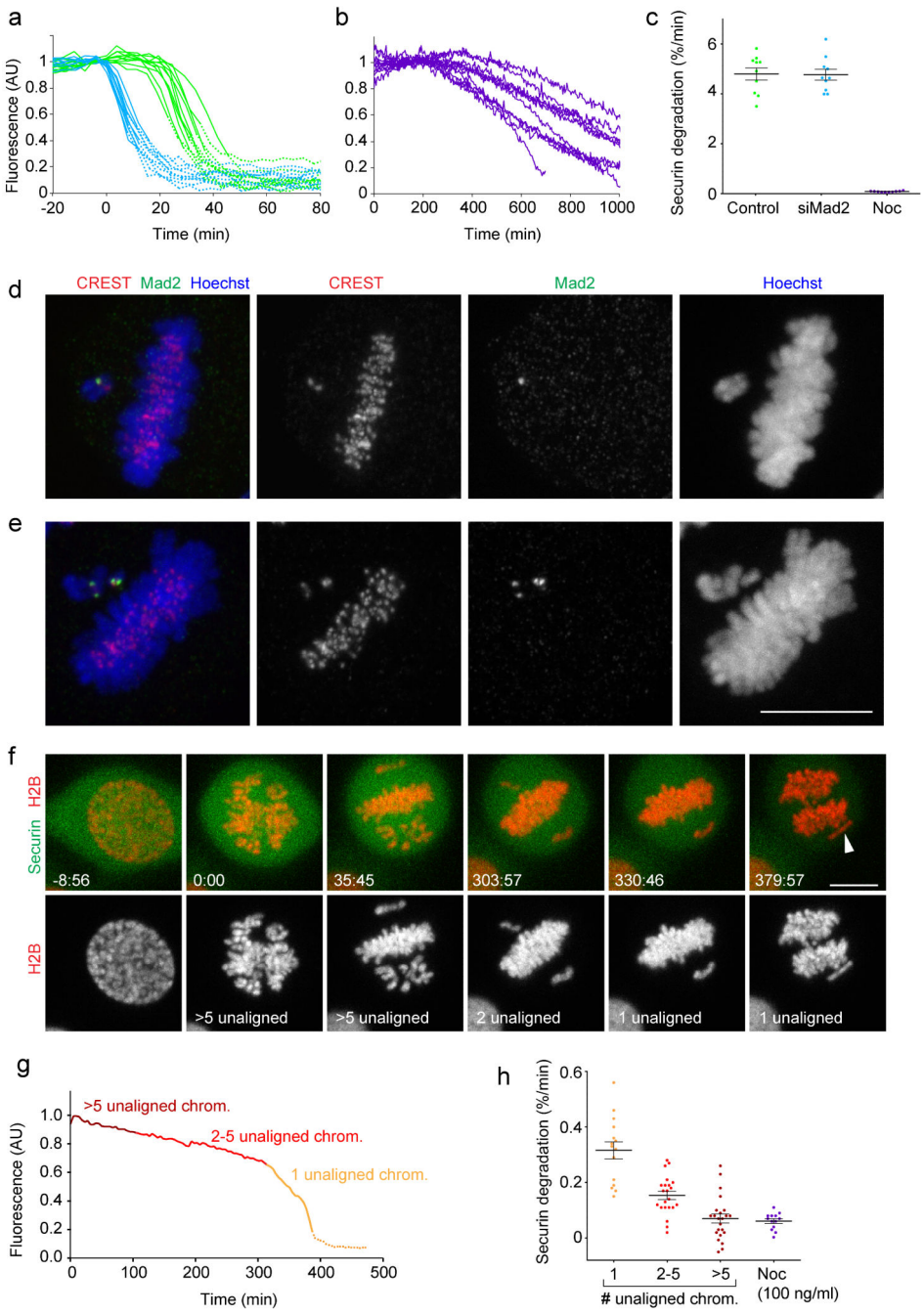

Figure 5. The inhibitory strength of the SAC correlates with the number of unaligned chromosomes

(**a**) Securin-mEGFP degradation rates peak briefly before anaphase onset. HeLa cells expressing H2B-mCherry and securin-mEGFP were transfected with non-targeting siRNA (control, green curves), or with siRNA targeting Mad2 (blue), and imaged live 24 h after transfection. Total securin-mEGFP fluorescence was measured in individual cells (n = 10 per condition). Time = 0 min at prometaphase onset. Solid lines indicate pre-anaphase stages; dashed lines indicate post-anaphase stages. (**b**) Securin-mEGFP degradation was measured as in (a) in cells treated with 100 ng/ml nocodazole. (**c**) Securin-mEGFP

Europe PMC Funders Author Manuscripts

degradation rates for cells shown in (a, b) were determined by linear regression. Each dot represents one cell. (**d, e**) Low concentrations of nocodazole selectively induce Mad2 accumulation on unaligned chromosomes. Cells treated for 3-5 h with 25 ng/ml nocodazole were fixed and stained with anti-Mad2 and CREST antibodies (n = 34 cells). (d) Cell with a single unaligned chromosome that accumulated Mad2 on a single sister kinetochore. (e) Cell with two unaligned chromosomes, which each accumulated Mad2 on both sister kinetochores. (**f**) A HeLa cell expressing H2B-mCherry and securin-mEGFP was imaged by 3D-confocal microscopy in presence of 12 ng/ml nocodazole. Arrowhead indicates a single unaligned chromosome during anaphase. Time = 0:00 min:s at prometaphase onset. (**g**) Total securin-mEGFP was measured as in (a) for the cell shown in (f). Dashed line indicates post-anaphase stages. See Supplementary Fig. S5 for four more examples and raw measurements. (**h**) Securin-mEGFP degradation was measured in 26 cells treated with 6, 12 or 25 ng/ml nocodazole, using linear regression at different time intervals (each dot represents one measurement that relates to a specific number of unaligned chromosomes, as illustrated in (g)). 13 control cells were treated with 100 ng/ml nocodazole. Error bars indicate mean ± s.e.m. Bars: 10 μm.